IET Nanobiotechnology

*Special Issue: Selected Papers from The International Conference on Nanomaterials and Nanotechnology 2015*

# Synthesis and characterization of MWCNT/$TiO_2$/Au nanocomposite for photocatalytic and antimicrobial activity.

ISSN 1751-8741
Received on 25th March 2016
Revised 8th October 2016
Accepted on 3rd November 2016
E-First on 11th January 2017
doi: 10.1049/iet-nbt.2016.0072
www.ietdl.org

*Viswanathan Karthika[1], Ayyakannu Arumugam[2]* ✉

[1]*Department of Nanoscience and Technology, Alagappa University, Karaikudi 630 003, Tamil Nadu, India*
[2]*Department of Botany, Alagappa University, Karaikudi 630 003, Tamil Nadu, India*
✉ *E-mail: sixmuga@yahoo.com*

**Abstract:** A novel combination of titanium oxide ($TiO_2$)/gold (Au)/multiwalled carbon nanotubes (MWCNTs) nanocomposite (NC) was synthesised by sol– gel method. MWCNT functionalisation by modified Hummers method. $TiO_2$/Au nanoparticles (NPs) were synthesised by biological method using *Terminalia chebula* bark extract. MWCNT/$TiO_2$/Au NC samples were characterised by X-ray diffraction, ultraviolet–visible–diffuse reflectance spectra, microRaman, scanning electron microscopy and high-resolution-transmission electron microscopy analyses. The photocatalytic performance of the obtained for NC toward the decomposition of congo-red and the antimicrobial activity for inhibition of Gram positive (*Bacillus subtilis, Streptococcus pneumonia* and *Staphylococcus aureus*), Gram negative (*Shigella dysenderiae, Proteus vulgaris* and *Klebsiella pneumonia*) and fungal strains have been evaluated and the results are compared with positive control ampicillin. The metal and metal–oxide NPs have a lower sorption capacity. The herbicidal bond to the tested CNTs by the combination of electron donor–acceptor interactions and hydrogen bonds. In particular, the dispersion of NC and control of sodium borohydride, it has more efficient effect on the photodegradation and antibacterial activity of positive control of ampicillin. The NC material has exhibited maximum photodegradation and antibacterial activity results of zone of inhibition when compared with control samples.

## 1 Introduction

The use of nanomaterials has been enormously increased in recent years leading to the development of a new generation technologies for environmental and public health production. The nanotechnology has the potential to create novel and effective in situ treatment technologies for the control of water pollution, ground water remediation, portable water treatment and air quality control [1]. Semiconductor and metal nanoparticles (NPs) are attracting much attention because of their shape- and size-dependent optical, electrical and catalytic properties [2]. The properties of metal NPs are significantly influenced by the external interactions with solid support materials and they acquire new composite materials with novel catalytic properties. Photocatalysis using semiconductor–metal nanocomposite (NC) materials and an advanced oxidation or reduction process have been developed in recent years [3]. Titanium oxide ($TiO_2$) is the principal catalyst for almost all types of photocatalysis reaction. However, it has photoactive wavelengths of below 400 nm due to its relatively large bandgap energy (3.2 eV). $TiO_2$ has been widely applied in heterogeneous photocatalysis inducing water purification [4–6], hydrogen production [7–9] and air detoxification [10, 11], owing to its high stability, non-toxicity and relative abundance [12].

The photocatalytic efficiency of $TiO_2$ was successfully enhanced by engineering the crystal structure [13–15]. $TiO_2$ and gold NPs (Au NPs) were found to be highly active for the catalytic oxidation of carbon monoxide. The Au NPs act as an electron sink during the photo-induced charge separation process at the $TiO_2$ by promoting the interfacial charge transfer process and reducing the charge recombination rate. Hence, the $TiO_2$–Au NC materials find a wide range of applications in the photocatalysis [16–19], dye sensitised solar cells [20], photo-electrochemical cells [21] and sensors [22]. Carbon nanotubes (CNTs) represent advanced materials due to their high surface area, good thermal stability and resistance; have been proposed as compounds for enzymatic sensors [23], DNA probes [22] and solid phase extraction [24]. Multiwalled CNTs (MWCNTs) are tubular graphene sheets, with diameters of 2–100 nm, rolled up into concentric cylinders with a layer spacing of 0.3–0.4 nm. CNTs, owing to their excellent optical properties and electron transfer ability, have been widely reported as an important substrate that can improve the photoactivity of $TiO_2$ [25]. CNTs play two important roles in a photocatalysis as a photosensitiser that enables the photo-activation of $TiO_2$ under the visible (vis) light irradiation and as electron sinks that transfer the electron away from the $TiO_2$ particles after photo-excitation via the CNT–$TiO_2$ heterojunction. The electrons can subsequently trigger the photo-reaction by formation of reactive radicals such as superoxide radical ions $O_2$ and hydroxyl radicals OH [26]. CNTs–$TiO_2$ composite exhibits great photocatalytic activity with excellent vis light absorption and unique electron charge transfer ability. MWCNT/$TiO_2$ core–shell NC exhibits the potential photocatalyst for reduction of $CO_2$ into methane [27]. MWCNT/$TiO_2$ NC displays good antibacterial activity under the ultraviolet (UV) light [28]. These composites were obtained most commonly using sol–gel [28] and other approaches such as chemical vapour deposition, functionalisation with titanium precursor [29] and solvothermal.

*Terminalia chebulla* (*T. chebulla*) is a species of Terminalia, native to southern Asia from India and Nepal East to southeastern china and South to Sri lanka, Malaysia and Vietnam. Chemical compounds present in *T. chebulla* bark extract such as gallic acids called chebulin, other phenolic compounds including ellagic acid, 2,4- chebulyl-$\beta$-D glucopyranose, chebulinic acid, ethyl gallate, punicalagin, terflavin A, terchebin tannic acid and luteic acid [30]. Hence, the present paper was aimed to synthesise $TiO_2$–Au NPs in the presence of *T. chebulla* as reducing agent. To the best of authors knowledge, this is the first study on *T. chebulla*-based $TiO_2$–Au NPs.

In the present paper, MWCNT/$TiO_2$/Au NC was synthesised by sol–gel method and the mass ratio of MWCNT to $TiO_2$/Au NPs was 1:1 have been synthesised. Photocatalytic and antimicrobial activity of MWCNT/$TiO_2$/Au NC was also investigated.

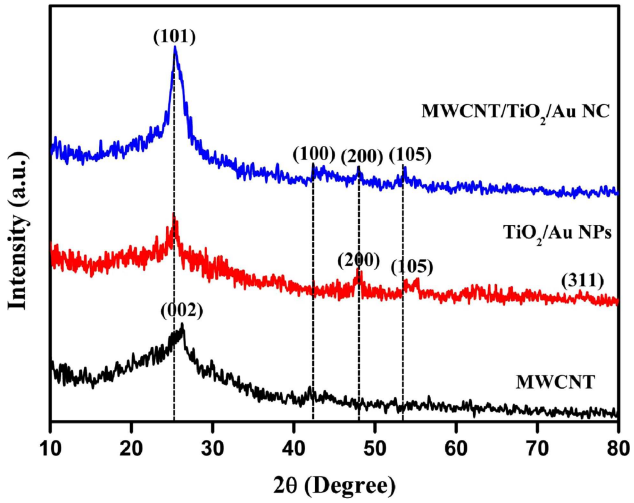


**Fig. 1** *XRD image of*
*(a)*MWCNT, *(b)*$TiO_2$–Au NPs, *(c)* MWCNT/$TiO_2$–Au NC

## 2 Materials and methods

### 2.1 Chemicals and reagents

Titanium isopropoxide [$C_{12}H_{28}O_4Ti$ (97%)], hydrogen tetrachloroaurate (III) trihydrate [$HAuCl_4.3H_2O$ (99.9%)], sulphuric acid ($H_2SO_4$), sodium nitrate ($NaNO_3$), potassium permanganate ($KMnO_4$), congo-red (CR) dye were obtained from Merck and Sigma-Aldrich chemicals (USA). All the solution was prepared using double distilled (DD) water.

### 2.2 Collection of plant and bark extract preparation

The *T. chebula* bark were collected from Endangered Medicinal Plants Conservation Center, Science Campus, Alagappa University, Karaikudi, Tamil Nadu, India.

*T. chebula* bark extract was prepared by taking 10 g in 250 ml Erlenmeyer flask with 100 ml of DD water and then boiled at 50–60°C for 5 min, finally filtered using Whatman No. 1 filter paper. The obtained bark extract was stored at room temperature for further usage.

### 2.3 Functionalisation of MWCNT

MWCNT was functionalised according to the modified Hummers method. Typically, 1 g of MWCNT and 0.5 g of $NaNO_3$ were mixed with 46 ml of concentrated $H_2SO_4$ (98%) in 250 ml conical flask. The mixture was stirred for 1 h in an ice bath. Subsequently, 3 g of $KMnO_4$ was added to the suspension under vigorous stirring. The rate of addition was carefully controlled to keep the reaction temperature lower than 20°C. After that, the mixture was removed from the ice bath and stirred at 35°C for 1 h. Then, 46 ml of DD water was slowly added with vigorous agitation. The diluted suspension was stirred for 30 min. At the end, 10 ml of hydrogen peroxide (30%) and 280 ml of DD water were added to the mixture and centrifuged with 10% Hydrochloric acid and DD water for several times. This washing process was repeated until the pH of the solution became neutral. After dried at 60°C, functionalised MWCNT was obtained as a grey powder.

### 2.4 Synthesis of $TiO_2$ with au NPs

In a typical reaction, 25 ml of bark extract was diluted with 475 ml of DD water. To the solution, 1 ml of (1 mM) Au chloride and 3 ml of (0.01 mM) $C_{12}H_{28}O_4Ti$ were added dropwise. The mixture was subjected to continuous vigorous stirring for 20 min. The colour change was observed from white to pink. Then, the mixture was allowed to continuous stirring at room temperature for 12 h. After stirring, the solution was heated at 80°C with stirring. At the time of colour change was observed from pink to coalescent red, clusters deposited on the bottom of the beaker. Soon after the reaction was stopped and prepared sample were collected and calcinated at 400°C for 3 h.

### 2.5 Synthesis of MWCNT/$TiO_2$/Au NC

The MWCNT/$TiO_2$/Au NC was synthesised by sol–gel method. In brief, 100 mg of functionalised MWCNT was dispersed in a 100 ml of ethanol. The solution was allowed to continuous stirring for 2 h to achieve uniform dispersion. Then, the above calcinated 100 mg $TiO_2$/Au powder was added and the mixture was subjected for sonication for 2 h. Followed by, the solution was allowed for continuous stirring for 12 h at room temperature. After sonicating, the solution was centrifuged several times and washed with DD water and ethanol. The precipitate was dried overnight at 60°C.

### 2.6 Materials characterisation

The synthesised NC characterised by X-ray diffraction (XRD) patterns were recorded using Bruker-AXS D8 ADVANCE with Cu K$\alpha$ radiation ($\lambda = 1.54178$ Å) from 10° to 80° at the scan speed of 0.2 $min^{-1}$, the operation voltage and current maintained at 35 kV and 200 mA. UV–vis–diffuse reflectance spectra (UV–vis–DRS) measured with a Hitachi U3010 spectrophotometer. Raman spectrum was recorded using laser Raman microscope, Raman-11 Nanophoton Corporation, Japan. The morphology of the calcined $TiO_2$/Au NPs and MWCNT/$TiO_2$/Au NC were examined by field emission-scanning electron microscopy (FE-SEM, Model: Hitachi S-4500). The particle size and crystalline nature were investigated by transmission electron microscopy (TEM) and selected area diffraction pattern (Tecnai Instruments), respectively.

## 3 Results and discussion

### 3.1 XRD analysis

In XRD analysis, three samples express similar patterns, which indicated the presence of Functionalized Multiwalled Carbon Nanotubes (FMWCNT), $TiO_2$/Au and MWCNT/$TiO_2$/Au NC materials and compared with the Joint Committee on Powder Diffraction Standards Card: 41487, 21-1272 and 04-0784 (Fig. 1). The XRD patterns exhibited at (002), (101), (100), (200) and (105) planes are indicates the presence of TiO2 /Au and MWCNT/$TiO_2$ /Au NC material. The crystalline size of the NC material was found to be 8.9 nm. The $TiO_2$ NPs were found to be in anatase phase.

### 3.2 UV–vis–DRS analysis

The synthesised NPs were characterised using UV–vis–DRS spectral analysis and it reveals that MWCNT/$TiO_2$/Au NCs exhibited a strong absorption peak at 304 nm for $TiO_2$, 254 nm for MWCNT and strong peak at 545 nm indicates the presence of Au NPs (Fig. 2). The continuous absorption band in the range of 400–800 nm is caused by the addition of carbon materials. Through the change of this kind of carbon materials affects the shape of the absorption curve. Red shift to higher wavelength was observed in the absorption edge of MWCNT/$TiO_2$/Au NCs, which may be attributed to electronic interaction between CNT and $TiO_2$.

### 3.3 Raman analysis

The Raman spectrum of MWCNT/$TiO_2$/Au NC exhibited characteristic peaks at 1334 and 1560 $cm^{-1}$ (Fig. 3). The D-band peak at 1325 $cm^{-1}$ is attributed to the disordered graphite structure (or) $sp^3$ hybridised carbon of the NT and the high-frequency G-band peak at 1560 $cm^{-1}$ represent to the splitting of the $sp^2$ hybridised carbon atoms (Fig. 4). The relatively increased $R$ value ($I_D/I_G$), which is the intensity of the D-band at 1334 $cm^{-1}$ G divided by the intensity of the G-band at 1580 $cm^{-1}$ of the functionalised carbon atoms. The manifestation of strapping $Eg$ mode at 144 $cm^{-1}$.

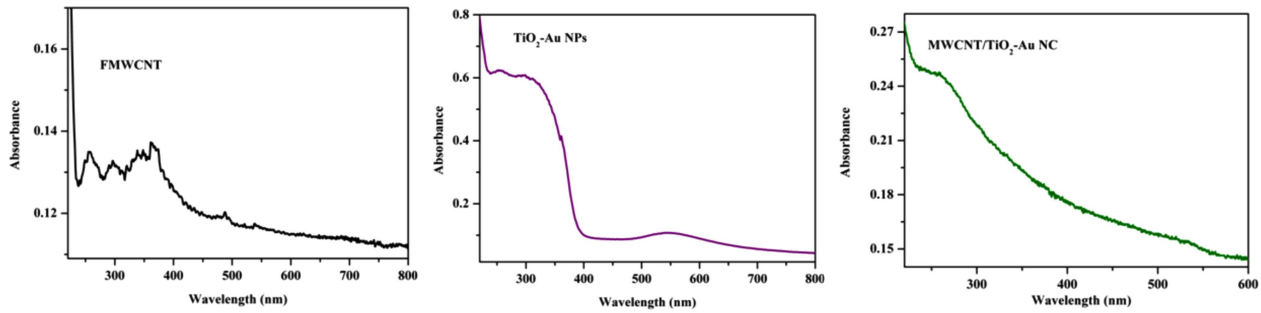


**Fig. 2** *UV–vis–DRS image of FMWCNT, $TiO_2$–Au NPs and MWCNT/$TiO_2$–Au NC (NC)*

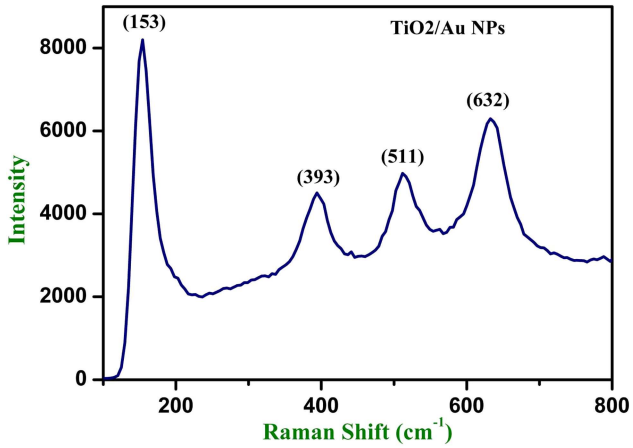


**Fig. 3** *Raman analysis of $TiO_2$–Au NPs*

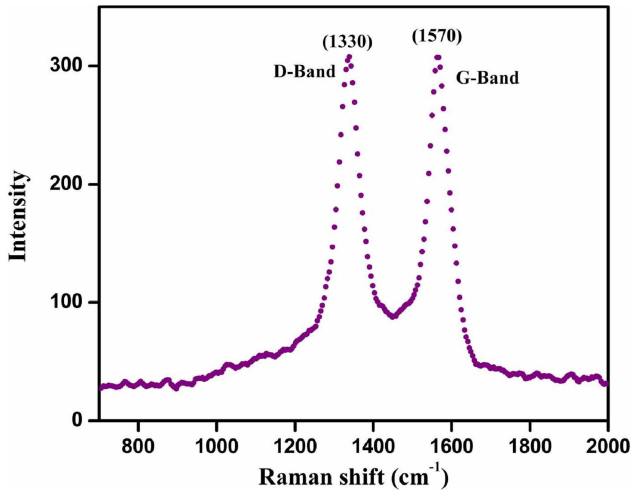


**Fig. 4** *Raman analysis of MWCNT*

### 3.4 SEM analysis

The surface morphology of the $TiO_2$/Au NPs and MWCNT/$TiO_2$/Au NC samples calcined at 400°C and examined via SEM analysis (Fig. 5). $TiO_2$/Au NPs were visualised to near spherical shape. The MWCNT/$TiO_2$/Au NC sample $TiO_2$/Au NPs that wrapped up around MWCNT. The diameter of the NC and NPs were measured to be in the range of 40–60 nm.

### 3.5 TEM analysis

The clear morphology and particle size of the calcined NCs were demonstrated by TEM analysis. The particle size was measured and it is in the range of 10 nm (Fig. 6). The calculated *d*-spacing values are corresponding to the *h k l* planes of (002), (101), (100) and (200) and also they are well associated with the XRD results.

### 3.6 Photocatalytic activity

The photocatalytic degradation of CR over the FMWCNT, $TiO_2$–Au NPs and NC was investigated. $TiO_2$–Au photocatalyst was illuminated with photons having energy greater than the bandgap energy, the photons will excite electron from the valance band of the $TiO_2$ into the conduction band (CB). The holes in the valance band were met with $OH^-$ and produce hydroxyl radicals. Therefore, the targeted pollution adsorbed on the surface of the catalyst was oxidised by ·OH. However, the excited electron–hole pairs may instead recombine [31]. The MWCNT act as a good electron acceptor and thereby facilitate the separation of the electron–hole to prevent their recombination. The mechanism of photocatalytic activity is valance band electrons ($e^-$) of titania, under the vis light irradiation are excited to CB, creating holes ($h^+$) in the valence band (VB). Normally, these charge carriers quickly recombine and only fraction, resulting in low reactivity. However, when $TiO_2$ was modified by the MWCNT/$TiO_2$/Au NC, the photocatalytic activity was enhanced. UV–vis spectroscopy was used to monitor the change in photocatalytic degradation of CR under vis light illumination (Fig. 7). *C* is the concentration of CR after vis light irradiation time and $C_0$ is the initial concentration of CR before light irradiation. CR, which has a major absorption peak

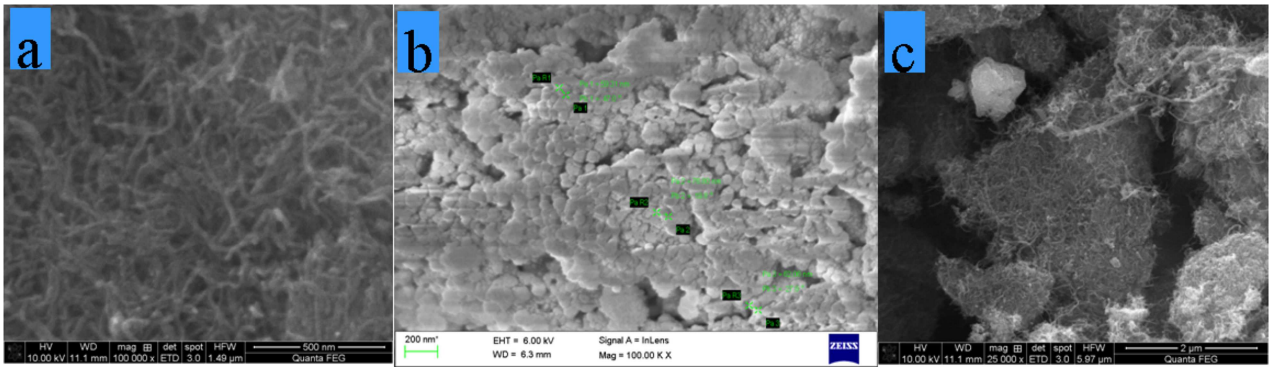


**Fig. 5** *SEM images of*
***(a)*** MWCNT, ***(b)*** $TiO_2$–Au NPs, ***(c)*** MWCNT/$TiO_2$–Au NC

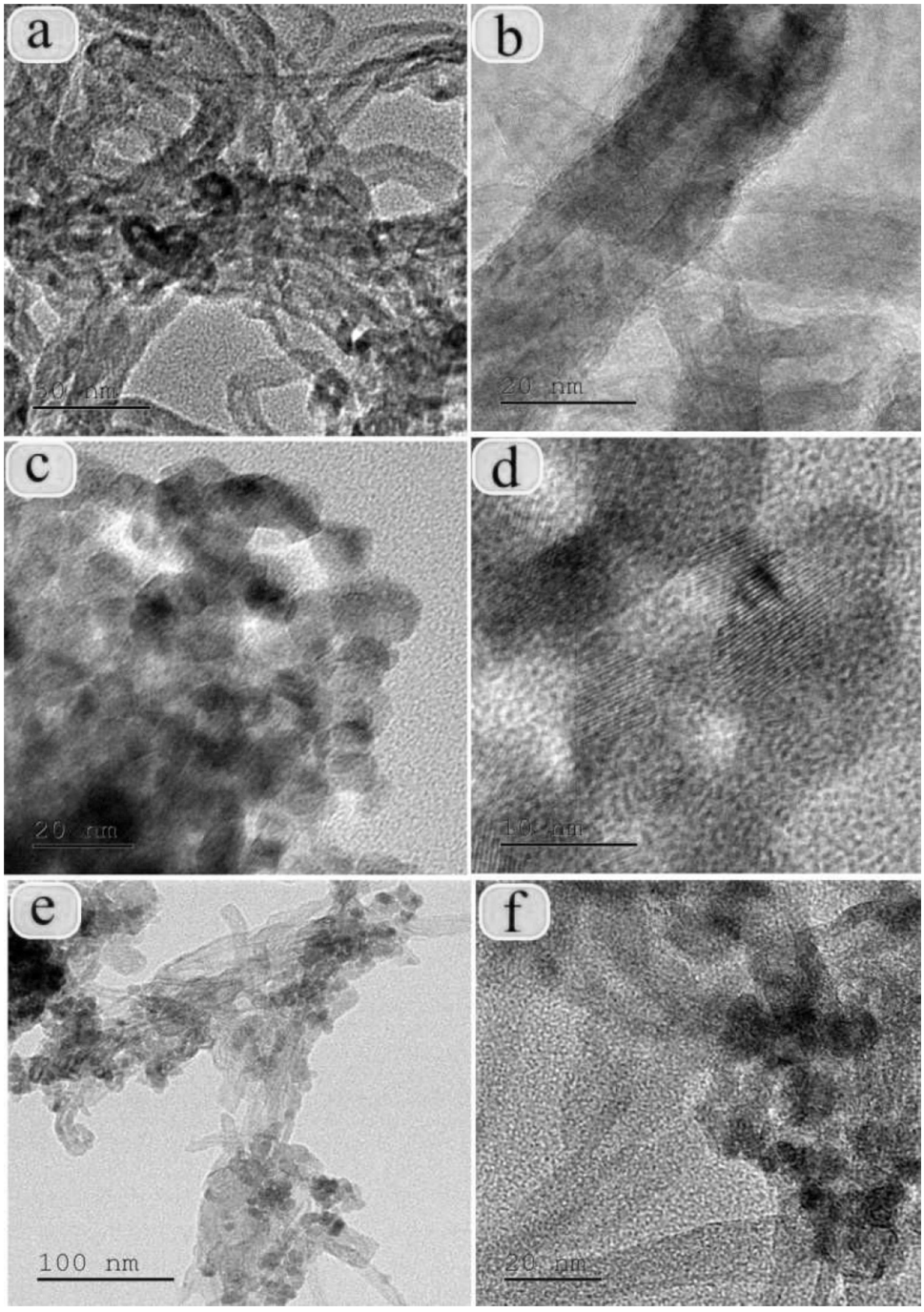


**Fig. 6** *TEM images of*
***(a, b)*** MWCNT, ***(c, d)*** $TiO_2$–Au NPs ***(e, f)*** MWCNT/$TiO_2$–Au NC

at 439 nm, is one of the most common organic pollutions in industrial waste water. About 40% degradation were observed, when CR + sodium borohydride (NaBH4) was applied. This is because of the slow recombination between CB electrons and VB holes in pure NaBH4, whereas 50 and 60% of photocatalytic activity was observed in FMWCNT and $TiO_2$–Au NPs, respectively. However, after introducing MWCNT/$TiO_2$/Au NC, the activity is remarkably enhanced and increased up to 87%. The kinetics of photocatalytic degradation of CR solution was investigated using a 2 mM initial concentration. A linear relationship between ln ($C_0/C$) and time (ln $C_0/C = kt$) was obtained. MWCNTs are similar to that of graphite, 4.7 eV, depending sensitively on the number of layers. $TiO_2$ NPs are in intimate contact with MWCNTs, the relative position of the MWCNT CB edge permits the transfer of electrons from $TiO_2$ surface, allowing charge separation, stabilisation and recombination. The excited electrons can be shuttled freely along the conducting network of MWCNTs and subsequently transfer to the surface to react with water and oxygen to yield hydroxyl radical, which would oxidise CR. Electrons excited by high-energy photons were transferred into the CNTs, and holes remained on the $TiO_2$ to form $OH^{\cdot}$ species, and then participated in the subsequent redox reactions. The outstanding electron accepting and trapping properties of CNTs helped retard or curb the recombination of electron–hole pairs, leading to formation of much more radical species [32, 33]. The NC exhibited better performance for the photodegradation of CR than the FMWCNT and $TiO_2$–Au NPs. This may be caused by the high surface area of the MWCNT, which can facilitate the separation of electron–hole pairs at MWCNT/$TiO_2$–Au interfaces. This indicates that the photocatalytic degradation of CR follows pseudo-first-order kinetics. Finally, photocatalytic activity of MWCNT/$TiO_2$/Au NC was achieved. Even though, photocatalytic activity of

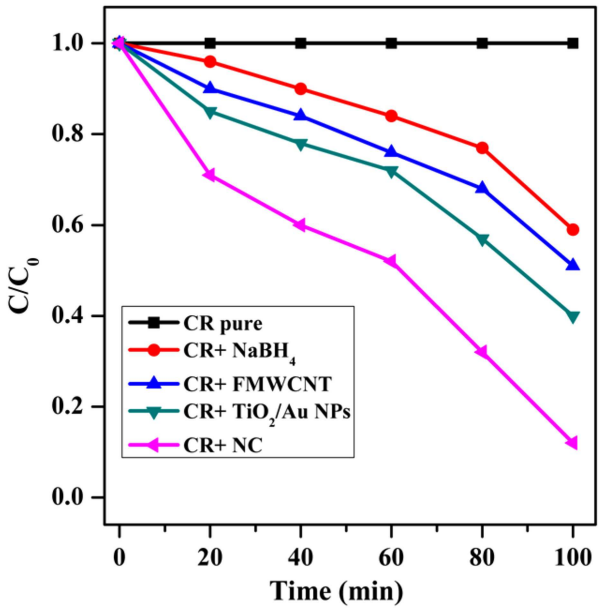


**Fig. 7** *Photocatalytic activity of CR*

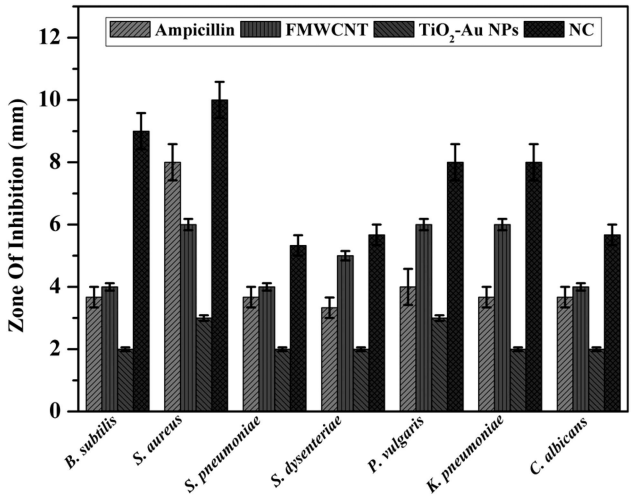


**Fig. 8** *Antimicrobial activity of ampicillin, FMWCNT, $TiO_2$–Au NPs and NC*

**Table 1** Antimicrobial activity zone of inhibition in millimetres

| Microbial name | Ampicillin | FMWCNT | $TiO_2$–Au NPs | NC |
|---|---|---|---|---|
| *B. subtilis* | 3.67 | 4 | 2 | 9 |
| *S. aureus* | 8 | 6 | 3 | 10 |
| *S. pneumoniae* | 3.6 | 4 | 2 | 5.3 |
| *S. dysenderiae* | 3.3 | 5 | 2 | 5.6 |
| *P. vulgaris* | 4 | 6 | 3 | 8 |
| *K. pneumoniae* | 3.6 | 6 | 2 | 8 |
| *C. albicans* | 3.6 | 4 | 2 | 5.6 |

MWCNT/$TiO_2$ and $TiO_2$/Au has been reported [32, 33]; this is the first report on photocatalytic activity of MWCNT/$TiO_2$–Au NC.

### *3.7 Antimicrobial activity*

The antimicrobial activity of ampicillin, FMWCNT, $TiO_2$–Au and NC against human and plant pathogenic bacterial and fungal strains were investigated (Fig. 8, Table 1). Antimicrobial properties zone of inhibition viable bacterial and fungal result was reasonably expectable because either CNTs (or) $TiO_2$ have antimicrobial properties as reported before [28]. Several recent studies suggest that peptide or lipid NTs can penetrate through cell membranes because of their cylindrical shape and high aspect ratio and lead to cell death. Owing to similarities in geometry, functionalised CNTs were also able to penetrate cell membranes. Interestingly, results from molecular dynamics stimulations can be used to explain the higher antimicrobial activity of smaller diameter CNT in comparison with that of large diameter and concentrations of CNT. Most of the studies have calculated that the main mechanism for the death of microbial effect of $TiO_2$ photocatalysis was $HO^{\cdot}$ attack and lipid peroxidation reaction [34]. These antifungal results suggest the NCs samples may affect cell functions and finally cause the increase of nucleic acid contents.

## 4 Conclusions

In this paper, MWCNT/$TiO_2$/Au NC was synthesised by simple sol–gel method and the synthesised NC was characterised by XRD, UV–vis–DRS, Fourier transform infrared spectroscopy, SEM and TEM analyses. XRD analysis exhibited the formation of MWCNT, $TiO_2$/Au and MWCNT/$TiO_2$/Au NC phases. UV–vis–DRS exhibited a red shift on absorption edge toward vis region in the NC. The synergistic effect emanates from the intimate contact between the MWCNT and $TiO_2$–Au NPs as evidence from the SEM and high-resolution-TEM images. Photocatalytic performance and antimicrobial activity of the NC against CR and bacterial and fungal strains under the vis light irradiation revealed the NC improves the photocatalytic and antimicrobial properties. This photocatalyst structure was unique and novel, which efficient catalytic performance was demonstrated by the photocatalytic decomposition of organic pollutions.

## 5 References


[1] Klabunde, K.J.: '*Nanoscale materials in chemistry*' (Wiley-Interscience, NJ, 2001)

[2] Hoffmann, M.R., Martin, S.T., Choi, W.Y., *et al.*: 'Environmental applications of semiconductor photocatalysis', *Chem. Rev.*, 1995, **95**, pp. 69–96

[3] Cozzoli, P.D., Curri, M.L., Agostiano, A.: 'Efficient charge storage in photoexcited $TiO_2$ nanorod-noble metal nanoparticle composite systems', *Chem. Commun.*, 2005, pp. 3186–3188, DOI: 10.1039/b503774c

[4] Mrowetz, M., Villa, A., Prati, L., *et al.*: 'Effects of Au nanoparticles on $TiO_2$ in the photocatalytic degradation of an azo dye', *Gold Bull.*, 2007, **40**, pp. 154–160

[5] Bannat, I., Wessels, K., Oekermann, T., *et al.*: 'Improving the photocatalytic performance of mesoporous titania films by modification with gold nanostructures', *Chem. Mater.*, 2009, **21**, pp. 1645–1653

[6] Bahnemann, W., Muneer, M., Haque, M.M.: 'Titanium dioxide-mediated photocatalysed degradation of few selected organic pollutants in aqueous suspensions', *Catal. Today*, 2007, **124**, pp. 133–148

[7] Bamwenda, G.R., Tsubota, S., Nakamura, T., *et al.*: 'Photoassisted hydrogen-production from a water ethanol solution; a comparison of activities of Au–$TiO_2$ and Pt–$TiO_2$', *J. Photochem. Photobiol.*, 1995, **89**, pp. 177–189

[8] Han, Z., Xufan, L., Tongxiang, F., *et al.*: 'Artificial inorganic leafs for efficient photochemical hydrogen production inspired by natural photosynthesis', *Adv. Mater.*, 2009, **22**, pp. 951–956

[9] Silva, C.G., Juarez, R., Marino, T., *et al.*: 'Influence of excitation wavelength (UV or visible light) on the photocatalytic activity of titania containing gold nanoparticles for the generation of hydrogen or oxygen from water', *J. Am. Chem. Soc.*, 2011, **133**, pp. 595–602

[10] Ao, C.H., Lee, S.C.: 'Indoor air purification by photocatalyst $TiO_2$ immobilized on an activated carbon filter installed in an air cleaner', *Chem. Eng. Sci.*, 2005, **60**, pp. 103–109

[11] Cao, Y.Q., He, T., Chen, Y.M., *et al.*: 'Fabrication of rutile $TiO_2$–Sn anatase $TiO_2$–N heterostructure and its application in visible-light photocatalysis', *J. Phys. Chem. C*, 2005, **114**, pp. 3627–3633

[12] Hernandez-Alonso, M.D., Fresno, F., Suarez, S., *et al.*: 'Development of alternative photocatalysts to $TiO_2$: challenges and opportunities', *Energy Environ. Sci.*, 2009, **2**, pp. 1231–1257

[13] Sun, Q.O., Xu, Y.M.: 'Evaluating intrinsic photocatalytic activities of anatase and rutile $TiO_2$ for organic degradation in water', *J. Phys. Chem. C*, 2010, **114**, pp. 18911–18918

[14] Andersson, M., Osterlund, L., Ljungstrom, S., *et al.*: 'Preparation of nano size anatase and rutile $TiO_2$ by hydrothermal treatment of microemulsions and their activity for photocatalytic wet oxidation of phenol', *J. Phys. Chem. B*, 2002, **106**, pp. 10674–10679

[15] Pan, J., Liu, G., Lu, G.M., *et al.*: 'On the true photoreactivity order of {001}, {010}, and {101} facets of anatase $TiO_2$ crystals', *Angew. Chem., Int. Ed.*, 2011, **50**, pp. 2133–2137

[16] Subramanian, V., Wolf, E.E., Kamat, P.V.: 'Influence of metal/ metal ion concentration on the photocatalytic activity of $TiO_2$Au composite nanoparticles', *Langmuir*, 2003, **19**, pp. 469–474

[17] Orlov, A., Chan, M.S., Jefferson, D.A., *et al.*: 'Photocatalytic degradation of water-soluble organic pollutants on $TiO_2$ modified with gold nanoparticles', *Environ. Technol.*, 2006, **27**, pp. 747–752
[18] Pradhan, S., Ghosh, D., Chen, S.: 'Janus nanostructures based on Au–$TiO_2$ heterodimers and their photocatalytic activity in the oxidation of methanol', *ACS Appl. Mater. Interfaces*, 2009, **1**, pp. 2060–2065
[19] Gopinath, K., Kumaraguru, S., Bhakyarj, K., *et al.*: 'Eco-friendly synthesis of $TiO_2$, Au and Pt doped $TiO_2$ nanoparticles for dye sensitized solar cell applications and evaluation of toxicity', *Superlattices Microstruct.*, 2016, **92**, pp. 100–110
[20] Subramanian, V., Wolf, E.E., Kamat, P.V.: 'Catalysis with $TiO_2$/gold nanocomposites. Effect of metal particle size on the Fermi level equilibration', *J. Am. Chem. Soc.*, 2004, **126**, pp. 4943–4950
[21] Cheng, J., Zhao, J., Tu, Y., *et al.*: 'Sensitive DNA electrochemical biosensor based on magnetite with a glassy carbon electrode modified by multi-walled carbon nanotubes in polypyrrole', *Anal. Chim. Acta*, 2005, **533**, pp. 11–16
[22] Wang, J.: 'Nanomaterial-based electrochemical biosensors', *Analyst*, 2005, **26**, pp. 421–426
[23] Zhou, Q., Ding, Y., Xiao, J.: 'Simultaneous determination of cyanazine, chlorotoluron and chlorbenzuron in environmental water samples with SPE multiwalled carbon nanotubes and LC', *Chromatographia*, 2007, **65**, pp. 25–30
[24] Feng, W., Feng, Y., Wu, Z., *et al.*: 'Optical and electrical characterizations of nanocomposite film of titania adsorbed onto oxidized multiwalled carbon nanotubes', *J. Phys. Condens. Matter*, 2005, **17**, pp. 43–61
[25] Bouazza, N., Ouzzine, M., Lillo-Ródenas, M.A., *et al.*: '$TiO_2$ nanotubes and CNT–$TiO_2$ hybrid materials for the photocatalytic oxidation of propene at low concentration', *Appl. Catal. B*, 2009, 92, pp. 377–383
[26] Yu, J., Ma, T., Liu, S.: 'Enhanced photocatalytic activity of mesoporous $TiO_2$ aggregates by embedding carbon nanotubes as electron-transfer channel', *Phys. Chem. Chem. Phys.*, 2011, **11**, pp. 3491–3501
[27] Gui, M.M., Chai, S.P., Xu, B.Q., *et al.*: 'Enhanced visible light responsive MWCNT/$TiO_2$ core–shell nanocomposites as the potential photocatalyst for reduction of $CO_2$ into methane', *Sol. Energy Mater. Sol. Cells*, 2014, **122**, pp. 183–189
[28] Ashkarran, A.A., Fakhari, M., Mahmoudi, M.: 'Synthesis of solar photo and bioactive CNT–$TiO_2$ nanocatalyst', *RSC Adv.*, 2013, **3**, pp. 18529–18536
[29] Li, J., Zeng, H.C.: 'Nanoreactors; size tuning, functionalization, and reactivation of Au in $TiO_2$ nanoreactors', *Angew. Chem., Int. Ed.*, 2005, **44**, pp. 4342–4345
[30] Kumar, K.M., Sinhaa, M., Mandal, B.M., *et al.*: 'Green synthesis of silver nanoparticles using *Terminalia chebula* extract at room temperature and their antimicrobial studies', *Spectrochim. Acta A*, 2012, **91**, pp. 228–233
[31] Hamid, S.B.A., Tan, T.L., Lai, C.W., *et al.*: 'Multiwalled carbon nanotube/$TiO_2$ nanocomposite as a highly active photocatalyst for photodegradation of reactive black 5 dye', *Chin. J. Catal.*, 2014, **35**, pp. 2014–2019
[32] Zhao, D., Yang, X., Chen, C., *et al.*: 'Enhanced photocatalytic degradation of methylene blue on multiwalled carbon nanotubes–$TiO_2$', *J. Colloid Interface Sci.*, 2013, **398**, pp. 234–239
[33] Zeng, Q., Li, H., Duan, H., *et al.*: 'A green method to prepare $TiO_2$/MWCNT nanocomposites with high photocatalytic activity and insights into effect of heat treatment on photocatalytic activity', *RSC Adv.*, 2015, **5**, pp. 13430–13436
[34] Arumugam, A., Karthikayan, C., Haja Hameed, A.S., *et al.*: 'Synthesis of cerium oxide nanoparticles using *Gloriosa superb* L. leaf extract and their structural, optical and antibacterial properties', *Mater. Sci. Eng. C*, 2015, **49**, pp. 408–415